34th Annual International Conference of the IEEE EMBS
San Diego, California USA, 28 August - 1 September, 2012

Detection of Neovascularization in the Optic Disc Using An AM-FM Representation, Granulometry, and Vessel Segmentation

Carla Agurto*,†, Honggang Yu†, Victor Murray*, Marios S. Pattichis*, Simon Barriga†, Wendall Bauman††, Peter Soliz†

*Electrical and Computer Engineering Department, University of New Mexico, Albuquerque, New Mexico 87131
†VisionQuest Biomedical LLC, Albuquerque, New Mexico 87106 ††The Retinal Institute of South Texas, San Antonio, Texas 78209. Email: capaagri@unm.edu

***Abstract*— Neovascularization, defined as abnormal formation of blood vessels in the retina, is a sight-threatening condition indicative of late-stage diabetic retinopathy (DR). Ischemia due to leakage of blood vessels causes the body to produce new and weak vessels that can lead to complications such as vitreous hemorrhages. Neovascularization on the disc (NVD) is diagnosed when new vessels are located within one disc-diameter of the optic disc. Accurately detecting NVD is important in preventing vision loss due to DR. This paper presents a method for detecting NVD in digital fundus images. First, a region of interest (ROI) containing the optic disc is manually selected from the image. By adaptively combining contrast enhancement methods with a vessel segmentation technique, the ROI is reduced to the regions indicated by the segmented vessels. Textural features extracted by using amplitude-modulation frequency-modulation (AM-FM) techniques and granulometry are used to differentiate NVD from a normal optic disc. Partial least squares is used to perform the final classification. Leave-one-out cross-validation was used to evaluate the performance of the system with 27 NVD and 30 normal cases. We obtained an area under the receiver operator characteristic curve (AUC) of 0.85 by using all features, increasing to 0.94 with feature selection.**

Diabetic Retinopathy; Amplitude-modulation Frequency-modulation; Granulometry, Partial Least Squares

I. Introduction

Fifty percent of diabetics with type I and twenty percent with type II diabetes will develop proliferative diabetic retinopathy (PDR) sometime in their lives [1, 2]. PDR is defined by the presence of neovascularization. When neovascularization is present within 1 disc diameter (DD) of the optic disc, it is called neovascularization of the disc (NVD), which poses a serious threat to vision. In this paper, we describe a method to detect the presence of NVD. In the literature, there are many algorithms focused on the segmentation of the vasculature in fundus images, which are summarized in [3]. However, most of the research is applied to cardiovascular diseases and there only few studies focused on abnormalities in the vessels present in PDR [4]. To the best of our knowledge, only Goatman *et al*. have presented a method to automatically detect NVD [5] using a bottom-up approach to detect the new vessels. By using watershed lines and ridge strength measurements, they select vessel candidates from the papilla of the optic disc. Fifteen features such as shape, position, brightness, contrast, and density are extracted from each candidate. The final classification of 38 NVD and 71 normal cases is performed by using a support vector machine (SVM). Their method achieved an area under the ROC curve (AUC) of 0.91.

In this paper, we present a system to detect the presence of NVD. We segment the vasculature of both normal and abnormal vessels in the region of interest (ROI), which covers 1 DD centered in the papilla, and characterize the ROIs based on textural features and granulometry. Contrary to [5], our classifier is applied to the images and not to the candidate segments.

II. Data Description

The retrospective images were provided by the University of Texas Health Science Center, San Antonio (UTHSCSA). 57 macula- and optic disc-centered digital fundus photographs were used to train/test our algorithm. Among those images, 27 contain NVD and 30 are normal. The camera has a field of view of 60 degrees and the images have 2392x2048 pixels, resulting in a pixel footprint of 9 μm. All the images have different disc diameters ranging between 120 and 500 pixels. To facilitate processing, the images were resized to have a DD of 400.

III. Methodology

Fig. 1 shows the methodology used to detect the presence of NVD. First, a region of 1DD centered in the optic disc is selected from the green channel of a retinal image. Then the region is enhanced and the vessels are segmented through an adaptive process. In the next step, features are extracted by applying two approaches: amplitude-modulation frequency-modulation and granulometry. Finally, partial least squares is used to classify neovascularization on the optic disc. We explain each component in the following sections.

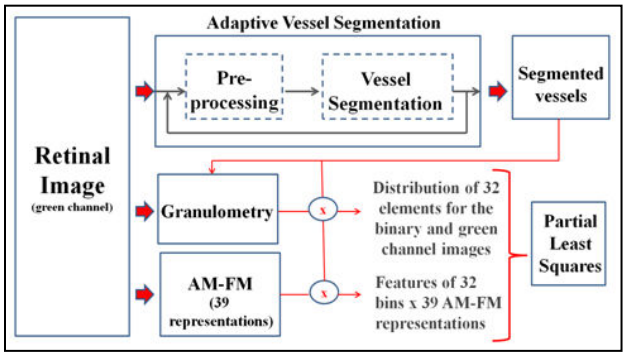

Figure 1. Block diagram of our approach to detect NVD.

A. *Adaptive Vessel segmentation*

In [6], we presented a method to segment retinal vasculature using multiscale enhancement with Frangi filters and second-order local entropy. Although this method achieved comparable or better results than other state of the art vessel segmentation algorithms, the same global procedure cannot be used to detect very fine vessels characteristic of NVD. Over segmenting the retinal vasculature would help detect fine vessels, but it would also produce a significant amount of noise. Therefore, we concluded that different regions of the image require different levels of pre-processing and, thus, local pre-processing methods are required.

The pre-processing stage consists of a shade correction method for illumination correction: contrast limited adaptive histogram equalization (CLAHE) for enhancement and anisotropic diffusion for noise reduction. We apply this procedure to small windows in an adaptive local approach. We apply the pre-processing to 200x200pixel regions with a 50 pixel overlap on both the vertical and horizontal axes.

Each region is repeatedly enhanced (CLAHE + anisotropic diffusion). A region being enhanced i consecutive times is said to have undergone the i-th level of enhancement. The correct level of enhancement for each region is adjusted based on the comparison of the segmentation of two consecutive levels of enhancement, in a manner described below. Fig. 2 shows the segmentation corresponding to three different levels of enhancement in a given region. The first level does not produce complete segmentation of vessels. By applying the second level, an adequate segmentation with almost no noise is achieved. However, the third level introduces more noise than relevant vessel segmentation.

We use the difference of the segmentation of level $i+1$ and level i to estimate the best level of enhancement. If the number of new pixels obtained by the segmentation of the last level ($i+1$) is too high, and these pixels are too spread in the region, we can conclude that the enhancement achieved on this last level has only added noise. On the other hand, if few new pixels are detected by the segmentation of the last level, it can be concluded that this level has not provided significant enough information for the segmentation. By taking into account these two cases, the parameters were empirically set for the adaptive vessel segmentation algorithm as follows. If the segmentation of level $i+1$ adds new pixels in the range of 5% to 10% of the number of pixels of the region (N=40000), with at least one connected component composed by more than 1% of N (400 pixels), level $i+1$ is preserved and the region undergoes another enhancement level. Otherwise, level i is selected as the optimal enhancement level of the analyzed region. Fig. 3 presents some results of the adaptive vessel segmentation applied to NVD cases.

In order to measure the performance of the adaptive vessel segmentation algorithm, a retinal grader marked the neovascularization in all the images. Using this ground truth, we found that more than 80% of the pixels containing NVD were correctly marked by our approach.

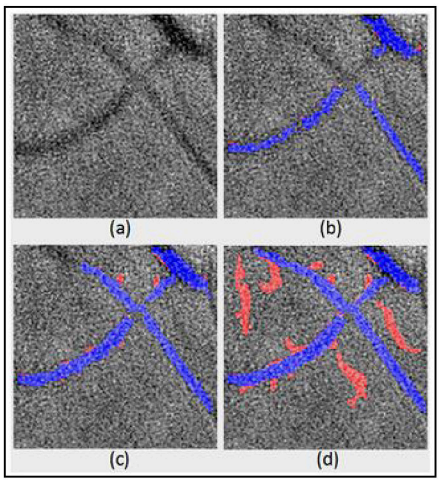

Figure 2. Segmentation of vessels for the ROI in a at 3 consecutive level of enhancement: b) level 1 c) level 2, and d) level 3. Color code: corrected segmented vessels in blue, uncorrected segmentation in red.

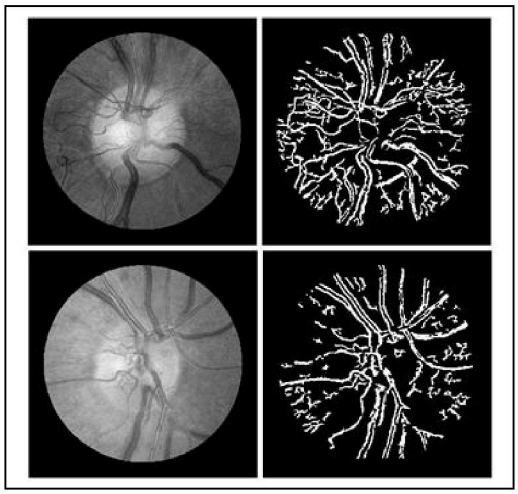

Figure 3. Segmentation of vessels for 2 optic discs with NVD.

B. *Amplitude-Modulation Frequency-Modulation*

Amplitude-Modulation Frequency-Modulation (AM-FM) [7] represents an image in terms of its instantaneous amplitude (IA) and frequency (IF) components as:

$$I(x,y) \approx \sum_{n=1}^{M} a_n(x,y)\cos\varphi_n(x,y) \qquad (1)$$

where M is the number of AM-FM components, $a_n(x,y)$ denote IA functions, and $\varphi_n(x,y)$ denote the instantaneous phase functions. For each AM-FM component, the IF is defined as the gradient of the phase φ_n. In terms of textural features three estimates of the AM-FM outputs are used for each component: IA, and the magnitude and angle of the IF.

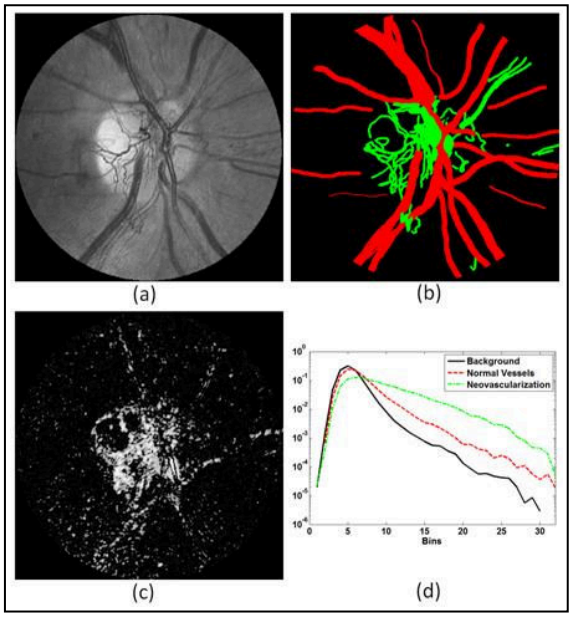

Figure 4. AM-FM representation of an image with NVD. a)Original image. b)Manually segmented vessel map (NVD in green). c)Instantaneous amplitude of (a) using high+medium frecuencies, d) Normalized histogram of the content of (c) for background, normal vessels, and NVD.

These AM-FM estimates were calculated at different frequency scales which correspond to the following bands of frequencies: High (H), Medium (M), Low (L), Very Low (VL), and Ultra Low (U). Then we merged them into 13 different combinations. Therefore, an image has 39 different AM-FM representations. Fig. 4c shows one of these representations: IA for H+M frequencies. In Fig 4d, we observe how the fine vessels of NVD are represented by the high-intensity pixels in this AM-FM output.

C. *Granulometry*

A Granulometry represents the size distribution of different objects in an image [8]. This methodology is based on applying a series of morphological opening operations of different size. In this approach, the difference between the original image and one of its openings is calculated, and the number of pixels is stored as one bin of a histogram.

In our approach, the objects to be analyzed are the vessels obtained in the binary map found using the methodology described in Section A. In order to generate the size distribution histogram, morphological opening operations with a disk-shaped structural element with radius (r) from 1 to 32 pixels are applied. By applying this approach to the image's green channel, we observed that small vessels characteristic of NVD are captured. For that reason, the same procedure is applied to the green channel image but in this case from each resulting image (original image minus its opening); the mean intensity value is calculated after masking them with the binary maps.

D. *Feature Extraction*

As explained in Section B, 39 different representations of AM-FM are obtained for each image. The vessel segmentation mask is applied to these estimates, and a 32-bin histogram is calculated with the remaining pixels. Therefore, we have 39 AM-FM types of features that generate 32x39 features.

In addition, we know that segmented vessels have different widths (e.g., NVD is characterized by having smaller vessel caliber). Thus, we used granulometry to extract two more types of features of 32 elements each, as specified in Section C. In total, 41 different types of features are obtained for each ROI.

E. *Classification*

The 41 features obtained in Section D are the inputs of a linear regression classifier based on partial least squares (PLS) [10]. The PLS classifier consists of two steps. First, the information is processed by each type of feature in order to reduce the dimensionality of our data. To select the best number of elements (factors) for reduction, mean square error (MSE) is calculated from different numbers of factors between the estimated classes and the classes of the training set images. The minimum MSE will determine the optimal number of factors for reduction. After reducing the dimensionality of the features, the matrices are concatenated in order to obtain a feature matrix to input to PLS, which will be used as a classifier.

F. *Feature Selection*

As in most classification systems, not all of the selected features significantly affect the results. Hence, we used the minimum MSE found for each type of feature as a metric for feature selection. This way, only the types of features that achieve a minimum MSE less than or equal to a threshold value ($MSE_{threshold}$) are used in our classifier. Fig. 5 shows how the performance of the classifier is affected when the $MSE_{threshold}$ decreases. If the value of $MSE_{threshold}$ is too low, and very few types of features are considered for the classifier, relevant information for the classifier is lost and the performance becomes unstable, as for $MSE_{threshold}$ = [0.16 0.20]. However, we found a steady performance for $MSE_{threshold}$ = [0.21 0.24] Based on this finding, the $MSE_{threshold}$ was set to 0.225.

In order to see the type of features that were used for the optimal $MSE_{threshold}$, we calculated the selection frequency in all iterations of the leave-one-out validation. 20 of the 41 features were selected. Features obtained with granulometry were always selected in the iterations. For the AM-FM estimates, IA was selected for combinations of scales where the L, VL, and U frequencies were present. On the other hand, combinations of scales selected for the IFm and IFangle have information from L, M, and H frequencies.

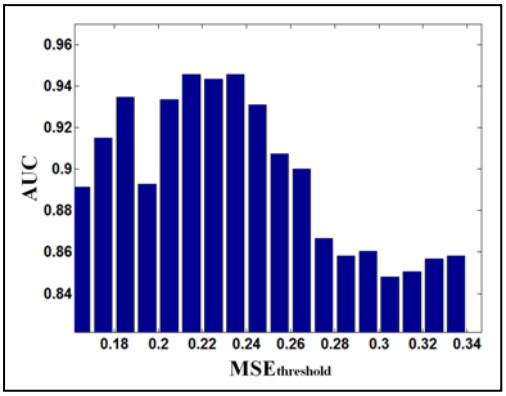

Figure 5. Bar plot of the performance of the classifier in terms of AUC vs. $MSE_{threshold}$.

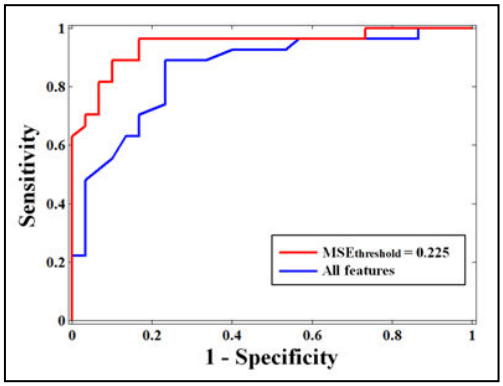

Figure 6. ROC curves for the classification of neovascularization.

IV. Results & Discussion

By using the 41 types of features described in this paper, an AUC of 0.85 with best sensitivity/specificity of 93%/60% was obtained in the classification of images with NVD. After feature selection with $MSE_{threshold\ =}$ 0.225, the AUC increases to 0.94 with best sensitivity/specificity of 96%/83%, as shown in Fig. 6.

It has been shown that feature selection using constrained MSE in PLS can be very useful in determining relevant types of features that increase the classifier's performance. However, the optimal MSE threshold can vary depending on the used training data. Future work would take this into account and automatically set the $MSE_{threshold}$ for each training set. The results obtained with this approach may surpass those obtained by using a fixed $MSE_{\ threshold}$.

By using constrained MSE in PLS, we have found that granulometry is a relevant feature. We have also found that the information from the IA is more useful in low frequencies, where vessels of regular caliber are captured with high intensity. On the other hand, the IFm and IFangle are preferred in the low to high frequencies, because neovascularization has components in those ranges of frequencies.

V. Conclusions

In this paper, we presented a novel method for detection of NVD, a sign of advanced stages of DR. The method achieved a performance AUC of 0.94.

By combining the bottom-up vessel segmentation approach and extracting textural features with AM-FM and granulometry, good performance results were obtained in the classification of NVD. This method could be used in a diabetic retinopathy screening system to increase the detection rate of sight-threatening conditions.

Although only a few samples were used to evaluate the performance of this approach, the results are promising, and are comparable with the ones obtained in [5]. Future work will include the addition of more images and types of features, and the optimization of parameters to increase the performance.

Acknowledgment

This work was supported by NEI grants EY020015 and RC3EY020749. The University of Texas Health Sciences Center in San Antonio provided the data used in this study.

References

[1] L. M. Aiello, L. P. Aiello, J. D. Cavallerano, "Ocular Complications of Diabetes Mellitus". In Kahn CR, Weir, GC, King GL, Jacobson AM, Moses AC, Smith RJ (ed.). Joslin's Diabetes Mellitus. Lippincott, Williams & Wilkins. Philadelphia, PA., pp. 901-924, 2005.

[2] R. Klein, B. E. Klein, S. E. Moss et al., "The Wisconsin Epidemiologic Study of Diabetic Retinopathy". X. Four-year incidence and progression of diabetic retinopathy when age at diagnosis is 30 years or more. *Arch Ophthalmol 1989*, vol. 107, pp. 244-249, 1989.

[3] R. J. Winder, P. J. Morrow, I. N. McRitchie, J. R. Baile, P. M. Hart, "Algorithms for digital image processing in diabetic retinopathy", *Comput Med Imaging Graph*., vol. 33, no. 8, pp. 608-22, 2009.

[4] P. H. Gregson, Z. Shen, R. C. Scott, and V. Kozousek, "Automated grading of venous beading," *Computers and Biomedical Research*, vol. 28, pp. 291–304, 1995.

[5] K. A. Goatman, A. D. Fleming, S. Philip, G. J. Williams, J. A. Olson, P. F. Sharp, "Detection of New Vessels on the Optic Disc Using Retinal Photographs,", *IEEE Transactions on Medical Imaging*, vol. 30, no. 4 pp. 972-979, 2011.

[6] H. Yu, S. Barriga, C. Agurto, G. Zamora, W. Bauman and P. Soliz, "Fast vessel segmentation in retinal images using multiscale enhancement and second-order local entropy", *Proc. SPIE 8315, 83151B*. 2012.

[7] V. Murray, P. Rodriguez, M.S. Pattichis, "Multi-scale AM-FM Demodulation and Reconstruction Methods with Improved Accuracy," *IEEE Transactions on Image Processing*, vol 19, no 5, pp. 1138-1152, 2010.

[8] Rafael C. Gonzales, Richard E. Woods, Digital Image Processing, second edition, Prentice Hall, 2002.

[9] C. Agurto, S. Barriga, V. Murray, et al., "Automatic detection of diabetic retinopathy and age-related macular degeneration in digital fundus images," *Invest Ophthalmol Vis Sci.*, vol. 52, no. 8, pp. 5862-5871, 2011.